

# Hysteretic enzyme adaptation to environmental pH: change in storage pH of alkaline phosphatase leads to a pH-optimum in the opposite direction to the applied change

Amrollah Behzadi, Rune Hatleskog, Peter Ruoff\*

*Stavanger College, School of Technology and Science, P.O. Box 2557 Ullandhaug, 4004 Stavanger, Norway*

Received 8 October 1998; received in revised form 26 January 1999; accepted 26 January 1999

---

## Abstract

The activity of alkaline phosphatase (AP) shows a change in optimum pH in the opposite direction to the applied change in storage pH. Typically, a change in storage pH from 9.8 to 8.5 results in a (reversible) change of the pH-optimum from 10.0 to 10.8. Protein fluorescence analysis shows that this response is probably due to conformational changes induced by the different storage conditions. As storage pH increases, a more ‘open’ or less ‘compact’ conformation is attained. Analysis of the diprotic model (a model which describes possible pH-responses of enzymes) indicates, that, as the AP conformation is getting more ‘open’, an increase in the dissociation of activity-regulating protons of AP occurs. This leads to a decrease in pH-optimum, precisely as found in the experiment. The prerequisite for such a response, however, is that the conformational adaptation to environmental assay pH is slow (hysteretic) when compared with assay time (400 s). The relaxation time of this adaptation was found to be in the order of 2 h. © 1999 Elsevier Science B.V. All rights reserved.

**Keywords:** Alkaline phosphatase; pH; Kinetics; Diprotic model; Protein fluorescence; Hysteretic enzymes

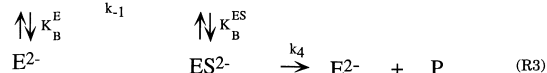
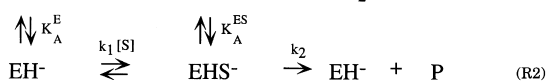
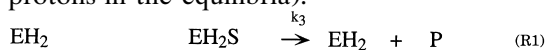
---

\* Corresponding author. Tel.: +47 51 831887; fax: +47 51 831750; e-mail: peter.ruoff@tn.his.no

**Abbreviations:**  $a_i$ ,  $\sigma_i$ , amplitude and dispersion parameters in  $f_i$  (Eq. (5)); AP, alkaline phosphatase;  $\text{EH}_2$ ,  $\text{EH}^-$ ,  $\text{E}^{2-}$ , different ionic enzyme species in diprotic model;  $\Phi(\lambda)$ , experimental fluorescence spectrum;  $f_i(\lambda)$ , gaussian function describing the tyrosine or tryptophan contributions of protein fluorescence (Eq. (5));  $\Phi_{\text{max}}$ , maximum fluorescence observed at wavelength  $\lambda_{\text{max}}$  (Fig. 5B);  $g$ , sum of three gaussian functions describing the overall protein fluorescence (Eq. (6));  $K_{A,B}^{\text{E(S)}}$ , proton dissociation constants in diprotic model (Eq. (2));  $k_i$ , rate constant ‘i’;  $\lambda_{\text{ex}}$ , excitation wavelength;  $\lambda_i^{\text{max}}$ , wavelength related to the maximum of function  $f_i$  (Eq. (5)); NR, nitrate reductase; P, product; S, substrate

## 1. Introduction

pH is an environmental parameter that affects the properties of all proteins and enzymes. Since the early work by Michaelis and Davidsohn [1], the occurrence of ‘bell-shaped’ activity curves has been explained in terms of diprotic models [2–7] in which the enzyme is considered as a weak 2-protic acid,  $\text{EH}_2$ . In these models, the key assumption is that  $\text{EH}^-$  is the main active enzyme species, while  $\text{EH}_2$  or  $\text{E}^{2-}$  are less active or inert. The assumed rapid equilibria between the different protonized and unprotonized enzyme species are described by the different dissociation constants  $K_{A,B}^{\text{E(S)}}$  (for making the appearance of the model less complex, we have omitted the protons in the equilibria):



The reaction between  $\text{EH}^-$  and substrate S may either be considered to be in a rapid equilibrium, or, alternatively, species  $\text{EHS}^-$  may be in a steady state. In both cases the same rate equation is obtained (see below). Whenever bell-shaped pH-profiles are observed the turnover number  $k_2$  is the dominating term compared to  $k_3$  and  $k_4$ . It should be realized, however, that the above model is a simplification, because substrate S could also bind to enzyme species  $\text{EH}_2$  and  $\text{E}^{2-}$  [8]. In addition, protons may become ‘sticky’, i.e. they may not easily exchange between enzyme species and the reaction medium. The situation where protons are sticky have been considered by Cleland [7].

An earlier study of the influence of pH on higher plant nitrate reductase (NR) showed the surprising result that NR’s pH-optimum moved in the opposite direction to the pH-change of the enzyme’s storage buffer [9]. The explanation of this effect involved the argument that at increasing (storage) pH values the enzyme’s conformation will become less ‘compact’ such that protons

from the enzyme’s surface become more easily dissociable into the surrounding solution. In terms of the diprotic model this is equivalent to an increase of the dissociation constants  $K_A^{\text{E(S)}}$  or  $K_B^{\text{E(S)}}$  leading both to a reduction in the corresponding  $\text{p}K_{A,B}^{\text{E(S)}}$  values and to a lower optimum pH. However, in order to reflect the change in  $K_{A,B}^{\text{E(S)}}$  by storage pH during the assay, the time scale of conformational adaptation to assay pH must be slow (hysteretic) compared with assay time [9].

We are not aware of earlier reports describing such an inverse relationship between storage pH and pH-optimum, but were wondering whether such behavior may also be observed for other enzymes. In this paper we report results for alkaline phosphatase (AP). The reason for choosing this enzyme was that AP is relatively stable, it is available in high purity and its kinetic mechanism [10,11] as well as the three-dimensional structure [12,13] is known. In this paper we show that, as for NR, APs pH-optimum also changes in the opposite direction to a pH perturbation in a storage buffer. The change in the pH-optimum is reflected by a corresponding change of the enzyme’s intrinsic fluorescence, which fits with the assumption that certain activity-related protons may become more easily dissociable with increasing storage pH.

## 2. Materials and methods

### 2.1. Enzyme and substrate working solutions

Calf intestine alkaline phosphatase (AP) (Boehringer Mannheim) was stored at 4°C (as recommended by the manufacturer). One unit of AP is the activity which hydrolyzes 1  $\mu\text{mol}$  *p*-nitrophenyl-phosphate in 1 min at 37°C at pH 9.8 [14]. The enzyme had a specific activity of 3141 units/mg protein. As a substrate working solution *p*-nitrophenyl phosphate (> 95%, Boehringer Mannheim) was dissolved in 0.1 M Tris of varying pH. Due to the relative high buffer concentration, no further adjustments of ionic strength were considered necessary. An enzyme working solution with an activity of 1 unit/1000  $\mu\text{l}$  in 0.1 M

Tris and varying pH was prepared. The initial substrate concentration in the reaction mixture was 1.14 mM. All pH measurements were made with a standard glass-electrode at 20°C.

Change of storage buffer containing enzyme was performed by ultrafiltration using a Centri-con 30 spin column (Amicon).

## 2.2. Spectroscopic methods

Prior to kinetic experiments and to allow equilibration to different storage pH values, the enzyme working solution was allowed to stand at 4°C for approximately 24 h. Kinetic experiments, however, were performed at 20°C. Initial velocities were measured spectrophotometrically (at 410 nm) as the amount of formed *p*-nitrophenol. The kinetic assay was performed by rapidly mixing 3 ml of substrate working solution with 100  $\mu$ l of enzyme working solution. The assay time was 400 s.

$K_M$  values were estimated from double-reciprocal plots for six different substrate concentrations in the range 19  $\mu$ M–1.14 mM. All double-reciprocal plots were linear. No practical differences were observed between simple or weighted [15] double reciprocal plots.

Fluorescence measurements were made with a Hitachi F-4500 spectrofluorimeter in a microcell (50  $\mu$ l). AP fluorescence emission spectra were recorded at an excitation wavelength of 280 nm and at an AP concentration of 1  $\mu$ M. The band pass was 5 nm for both excitation and emission wavelengths. To minimize the effect of fluctuations in the sample, AP emission spectra  $\Phi$  were obtained as the mean of 25 repetitive scans (CAT-mode of fluorimeter). The deconvolution of  $\Phi$  into a linear combination of three gaussian functions (see below) was performed by using KaleidaGraph (Macintosh version 3.0.2, Abelbeck Software, 1993). Three-dimensional emission/excitation spectra were constructed from single scans.

## 2.3. Adaptation kinetics to environmental pH change

We have investigated the time scale of the reversible adaptation in enzyme activity at an

assay of pH 10.0 when the storage buffer is rapidly changed from pH 10.0 to pH 7.3. For this purpose, 0.01 units of AP (dissolved in 200  $\mu$ l 0.1 M Tris, pH 10.0) were allowed to equilibrate for approximately 24 h at 4°C. After this period the enzyme was allowed to stand at 20°C for approximately 1 h. Ten microliters of the equilibrated AP solution was mixed with 90  $\mu$ l 0.1 M Tris (pH 5.5). The resulting pH of the mixture was found to be 7.3. After mixing, the enzyme activity slowly adjusted to the new environmental pH. To determine the time scale (relaxation time) of this adaptation, the activity was measured for various storage times by mixing 100  $\mu$ l of enzyme solution with 3 ml (pH 10.0) of substrate solution (see above).

## 2.4. Diprotic model

All protonization and deprotonization reactions are assumed to be in a rapid equilibrium.  $K_{A,B}^E$  and  $K_{A,B}^{ES}$  are the equilibrium (dissociation) constants of the protonized forms of the free enzyme and the enzyme substrate complex, respectively. The reaction velocity  $v$  in the diprotic model is the sum of velocities of reactions R1–R3:

$$v = k_2[\text{EHS}^-] + k_3[\text{EH}_2\text{S}] + k_4[\text{ES}^{2-}] = k_2[\text{EHS}^-] \left( 1 + \frac{k_3}{k_2} \cdot \frac{[\text{H}^+]}{K_A^{ES}} + \frac{k_4}{k_2} \cdot \frac{K_B^{ES}}{[\text{H}^+]} \right) \quad (1)$$

with

$$K_A^{E(S)} = \frac{[\text{H}^+][\text{EH}(\text{S})^-]}{[\text{EH}_2(\text{S})]}, \quad K_B^{E(S)} = \frac{[\text{H}^+][\text{E}(\text{S})^{2-}]}{[\text{EH}(\text{S})^-]} \quad (2)$$

Let  $[\text{E}]_0$  be the total enzyme concentration  $[\text{S}]$  the concentration of unbound substrate (which is taken as the total substrate concentration),

$$V_{\max} = k_2[\text{E}]_0, \quad K_M = \frac{k_2 + k_{-1}}{k_1},$$

$$f_{E(S)} = 1 + \frac{[\text{H}^+]}{K_A^{E(S)}} + \frac{K_B^{E(S)}}{[\text{H}^+]}, \quad \alpha = \frac{k_3}{k_2},$$

$$\beta = \frac{k_4}{k_2}, \text{ and } f_{\alpha\beta} = 1 + \alpha \frac{[H^+]}{K_A^{ES}} + \beta \frac{K_B^{ES}}{[H^+]}$$

The reaction velocity (Eq. (1)) will depend on pH and the parameters **a**:

$$\mathbf{a} = (a_1, a_2, \dots, a_7) \\ = (pK_A^E, pK_B^E, pK_A^{ES}, pK_B^{ES}, V_{\max}, \alpha, \beta) \quad (3)$$

Further algebra leads to:

$$v = v(\text{pH}, \mathbf{a}) = V_{\max} [\text{S}] \frac{f_{\alpha\beta}}{f_E K_M + f_{ES} [\text{S}]} \quad (4)$$

Parameters **a** were fitted to the experimental rate data by minimizing the mean square deviation  $\chi^2 = \sum_{\text{pH}} (v_{\text{exp}}(\text{pH}) - v(\text{pH}, \mathbf{a}))^2$  between experimental velocities  $v_{\text{exp}}(\text{pH})$  and  $v(\text{pH}, \mathbf{a})$ . Minimization of  $\chi^2$  is achieved by calculating the gradients  $\partial\chi^2/\partial a_i$  for a given starting set of parameters and by changing the parameters  $a_i$  iteratively along the steepest descent until gradients approach zero [16]. The  $K_M$  values were estimated experimentally and were not changed during curve-fitting. pH-optima were determined from the optimized  $v(\text{pH}, \mathbf{a})$  by numerical inspection.

### 3. Results

#### 3.1. pH-profiles

Fig. 1A shows the experimental velocities as a function of assay and storage pH. For storage pH values larger than 8.3 we observed ‘bell-shaped’ pH-profiles with a pH-optimum that decreases with increasing storage pH. The solid lines in Fig. 1A represent the fitted  $v(\text{pH}, \mathbf{a})$  function (Eq. (4)). Below storage pH 8.3, the pH-profile became monotonic (Fig. 1B,C). At an assay pH of 12.0 (or higher) a sudden drop in enzyme activity was found (Fig. 1C), which was probably due to partial denaturation of the enzyme. The maximum activity of AP occurs at a storage pH of approximately 10.8 with a pH-optimum of approximately 9.8/9.9. Increasing the storage pH above 10.8 results in a decrease of activity (Fig. 2A).

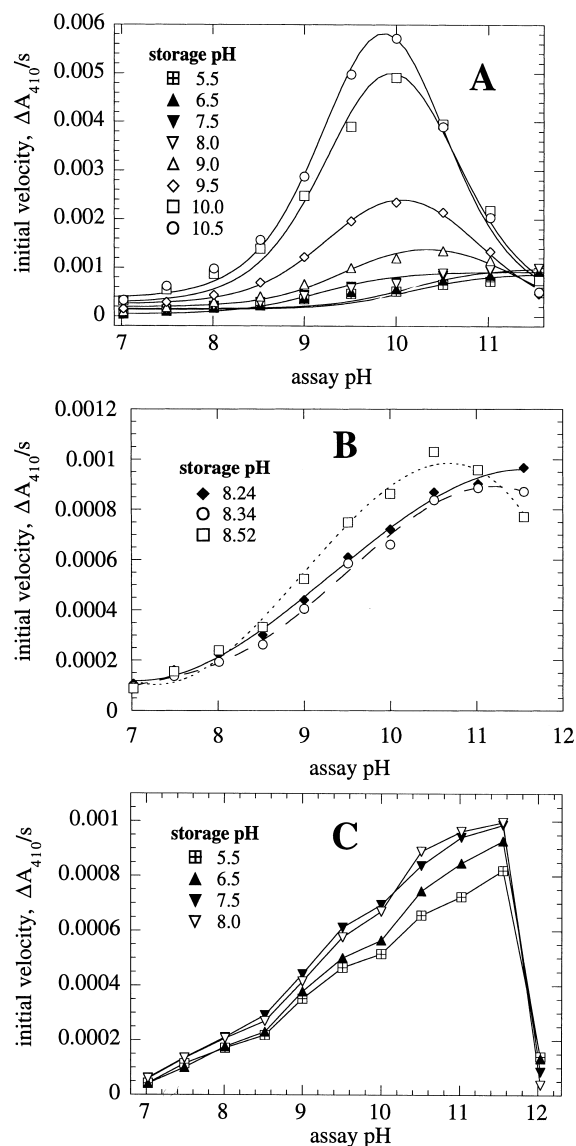


Fig. 1. (A) Initial velocities as a function of assay pH and storage pH. Solid lines represent optimized functions  $v(\text{pH}, \mathbf{a})$  (Eq. (4)). (B) By varying the storage pH from 8.52 to 8.24 the pH-response changes from a ‘bell-shaped’ form to a ‘monotonic’ profile. (C) At assay pH larger than 12.0 a sudden drop in activity is observed. Solid lines represent now only the connection between experimental data points.

Fig. 2B shows the variation of pH-optimum with changing storage pH. The abrupt change at storage pH  $\approx 8.2$  indicates the transition between ‘bell-shaped’ and ‘monotonic’ pH-profiles.

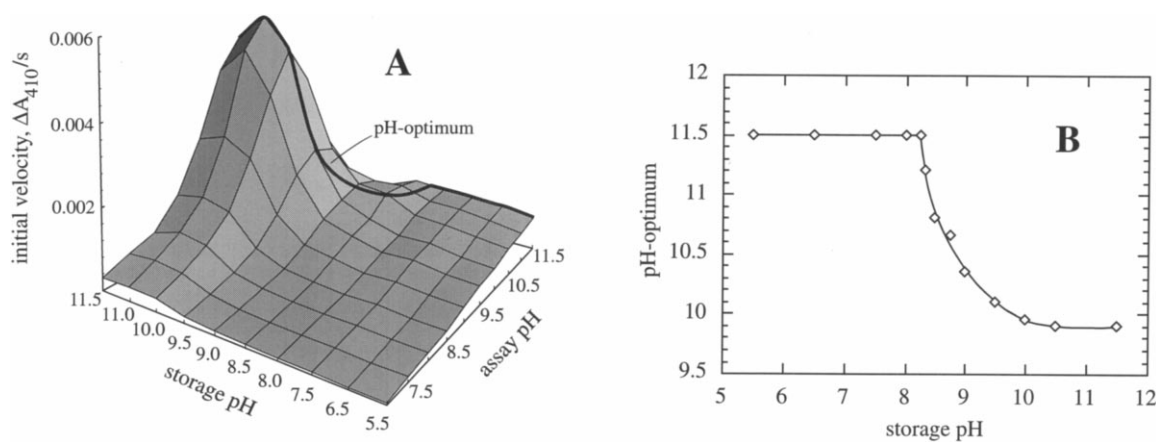


Fig. 2. (A) Three-dimensional view of the experimental velocities as a function of storage and assay pH. Solid line indicates the pH-optimum. (B) Determined pH-optimum as a function of storage pH. For storage pH values larger than 8.3 ‘bell-shaped’ pH-profiles are observed, where pH-optimum changes inversely with storage pH. In the range where a monotonic response is observed (Fig. 1C) the pH-optimum is set to 11.5.

Fitting Eq. (4) to the experimental data points leads to the optimized parameter set **a** (Eq. (3)). This set, however, changes with storage pH (Fig. 3). In the region of bell-shaped pH profiles (storage pH larger than 8.3), an increased storage pH leads to an increase of dissociation constants  $K_A^{ES}$ ,  $K_B^E$ , and  $K_B^{ES}$  (decrease in  $pK$ ) while there is only a slight variation in  $K_A^E$  (Fig. 3A). When storage pH is below 8.2, the  $pK_B^{E(S)}$ s attain high values indicating that the  $K_B^{E(S)}$  constants are practically zero. Also  $\alpha$  and  $\beta$  values show a clear change at storage pH 8.2/8.3 (Fig. 3B).  $V_{max}$  has its maximum at a storage pH of approximately 10.8 (Fig. 3C), but no abrupt changes are observed at storage pH  $\approx$  8.2. Fig. 3D shows the experimentally estimated  $K_M$  values (as  $pK_M$ ) as a function of storage pH.

### 3.2. Reversibility

Reversibility of the storage pH induced pH-profiles were tested by interchanging the storage buffer of two enzyme samples between pH 5.5 and pH 10.5. We found that the influence of storage pH on pH-profiles appear fully reversible (data not shown).

### 3.3. AP-fluorescence

We investigated AP’s intrinsic fluorescence to

see whether there is a correlation between possible conformational information and activity. The fluorescent part in the single chain of calf intestine AP consists of 4 tryptophan (W), 14 phenylalanine (F) and 20 tyrosine (Y) [17]. Fig. 4 shows the three-dimensional fluorescence spectrum of 1  $\mu$ M AP (0.1 M Tris, pH 7.5) in comparison with the corresponding spectra of tryptophan, phenylalanine, and tyrosine. Both the amino acids and protein fluorescence show two peaks. For AP, these peaks occur at  $\lambda_{ex} = 225$  nm and  $\lambda_{ex} = 280$  nm. Since the peak at the 280 nm excitation is smoother, we have studied the AP fluorescence at this wavelength. At  $\lambda_{ex} = 280$  nm phenylalanine (F) does not contribute to the observed emission (Fig. 5A). The tyrosine (Y) fluorescence is described well by a one-gaussian function  $f_i$ :

$$f_i(\lambda) = a_i \exp\left[-\sigma_i(\lambda - \lambda_i^{\max})^2\right] \quad (5)$$

in which  $a_i$  and  $\sigma_i$  are constants, and  $\lambda_i^{\max}$  is the wavelength related to the maximum of  $f_i$ . The tryptophan (W) fluorescence is described by a 2-gaussian fit, i.e. by a superposition of two  $f_i$  functions (Fig. 5A). Indeed, there are indications that the tryptophan fluorescence is a 2-component process [18].

The solid line in Fig. 5B shows the average of 25 repetitive emission spectra for AP stored at

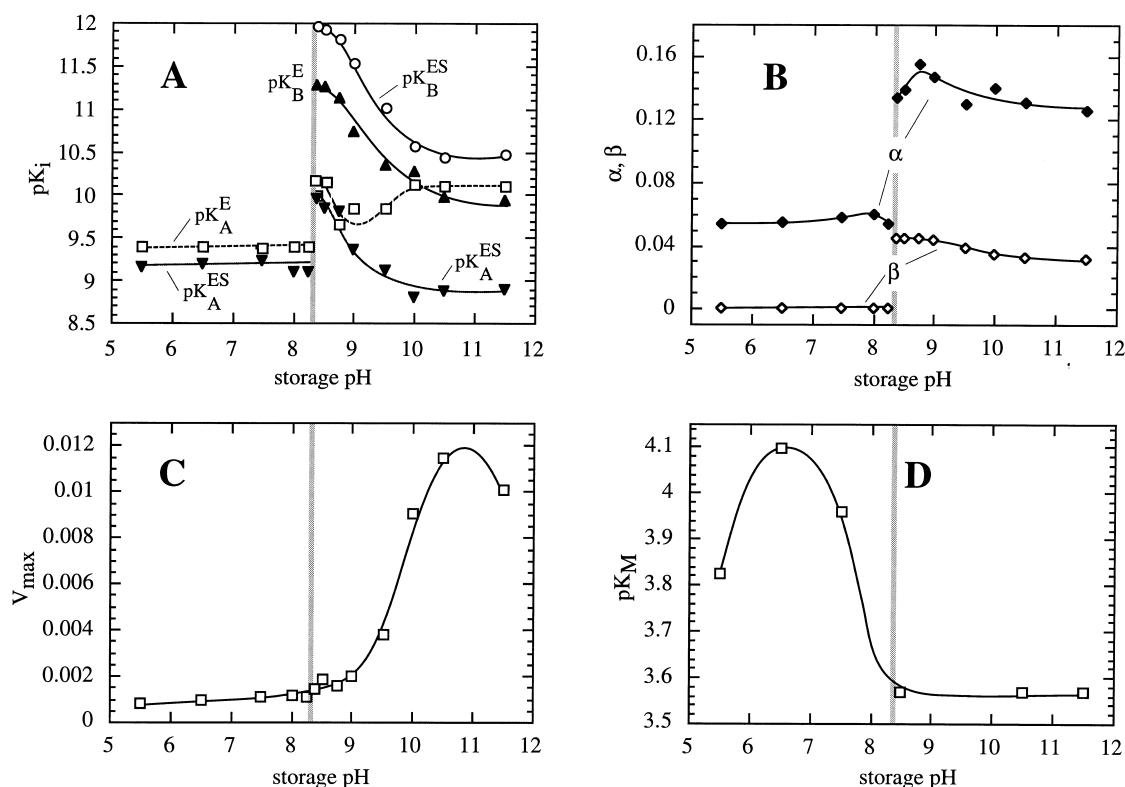


Fig. 3. (A)–(C) The change of optimized parameters  $\mathbf{a}$  in  $v(\text{pH}, \mathbf{a})$  (Eqs. (3), (4)) as a function of storage pH. (D) Experimentally determined  $\text{pK}_M$  values.

pH 7.5. A deconvolution of this spectrum into three gaussian functions  $g$

$$g = \sum_{i=1}^3 f_i \quad (6)$$

shows that there is practically a perfect fit between  $g$  and the experimental emission spectrum  $\Phi$ . This rather good description of the AP-fluorescence by the  $g$ -function (Eq. (6)) was observed for all spectra taken, independently of storage pH! As storage pH was changed, a change in the parameters  $a_i$ ,  $\sigma_i$  and  $\lambda_i$  (Eq. (5)) was also observed. Fig. 6A–C shows these changes for a series of storage pH values. Interestingly, we found a symmetrical change of amplitudes  $a_2$  and  $a_3$ , which seems to provide further evidence that  $f_2$  and  $f_3$  describe the same amino acid (W). Based on the previous observations [18] that tryp-

tophan fluorescence appears to be described by a 2-component process together with the 2-gaussian fit of tryptophan fluorescence, it is tempting to consider  $f_1$  as the contribution of tyrosine and  $f_2 + f_3$  as the tryptophan part to the AP emission spectrum.

Despite the fact that the experimental emission spectra  $\Phi$  are perfectly described by the  $g$ -function, the maximum fluorescence  $\Phi_{\max}$  and  $\lambda_{\max}$  (Fig. 5B) have been found to be subject to considerable fluctuations. From three repetitive measurements of the same set of AP solutions, the average uncertainty in  $\Phi_{\max}$  and  $\lambda_{\max}$  was estimated to be approximately 300–400 au (arbitrary units) and 1–2 nm, respectively. Fig. 6D shows  $\Phi_{\max}$  and  $\lambda_{\max}$  from the experimental data from which the  $a_i$ ,  $\sigma_i$  and  $\lambda_i$  of Fig. 6A–C were extracted. In addition, the experimental uncertainties in  $\Phi_{\max}$  and  $\lambda_{\max}$  are indicated. The trend

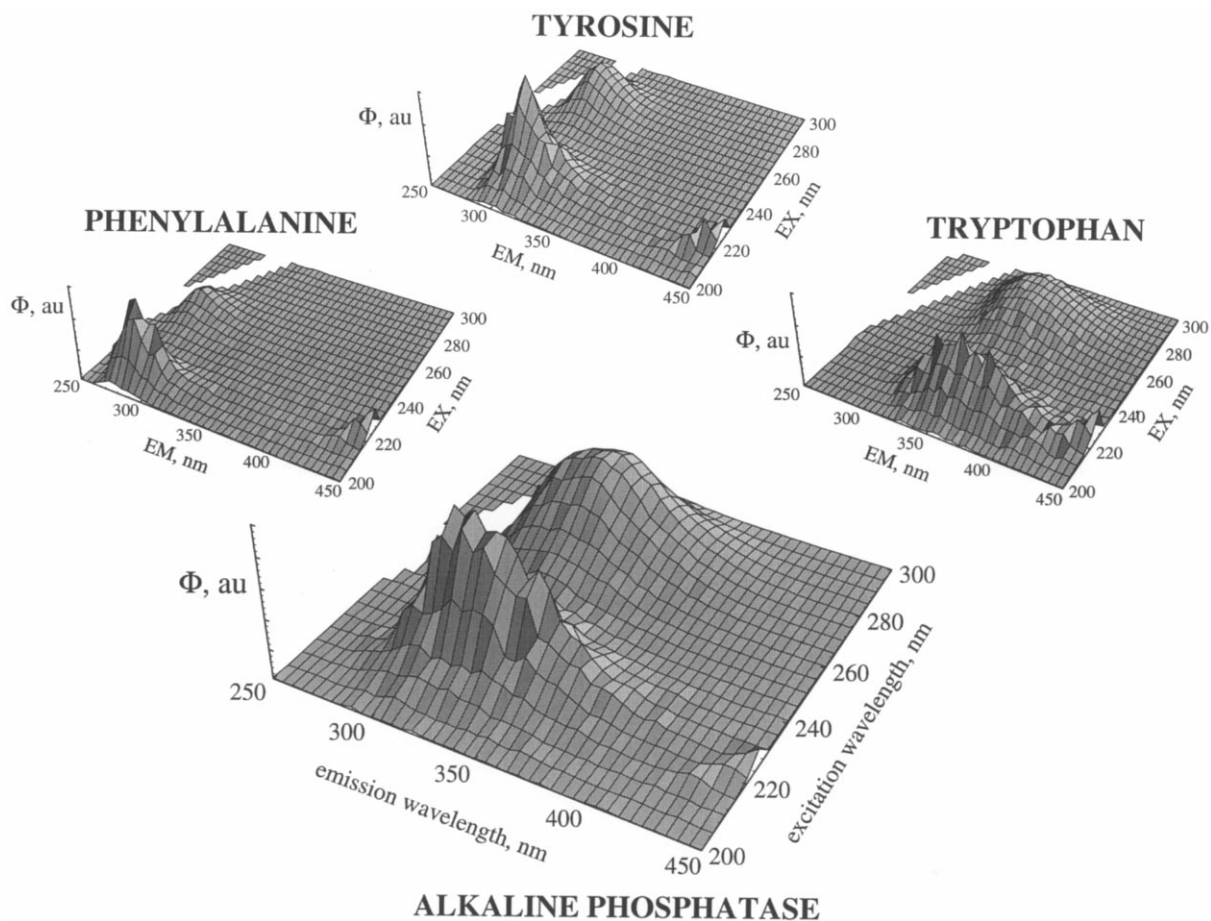


Fig. 4. Three-dimensional-fluorescence spectra of tyrosine, phenylalanine, tryptophan and AP at storage pH 7.5. The spectra were constructed from single scans (scan speed 30 000 nm/min) with a sampling interval of 5 nm. The white thick line indicates the region of Rayleigh scattering.

of  $\Phi_{\max}$  and  $\lambda_{\max}$  as a function of storage pH is a general decrease and increase, respectively. However, we always found an indication of two local maxima in  $\Phi_{\max}$  at storage pH  $\approx 7$  and  $\approx 10$  and a minimum in  $\lambda_{\max}$  at storage pH  $\approx 10$ . As storage pH becomes very high  $\lambda_{\max}$  is dramatically increasing and a corresponding decrease in  $\Phi_{\max}$  is observed.

#### 4. Discussion

As expressed in a review paper more than 30 years ago [19], the number of reports concerning the effect of pH on the activity of various alkaline phosphatases is legion. However, despite the large

amount of literature available on pH-effects on this and other enzymes, we have not been able to trace reports on inverse relationships between pH-optimum and storage pH. Both NR [9] and AP have in common that the substrate is present in a single ionic form 'S' which is not affected by the assay pH of the system (data not shown). For AP, the experimental 'bell-shaped' pH-profiles are well described by the diprotic model. The slight asymmetry in these profiles (Fig. 1A) indicates that the acid form of the enzyme also appears to be kinetically active. From the  $\alpha$  parameter (Fig. 3B), the activity of  $\text{EH}_2\text{S}$  (reaction channel R1) is approximately 12–16% of the activity of the main route (reaction channel R2).

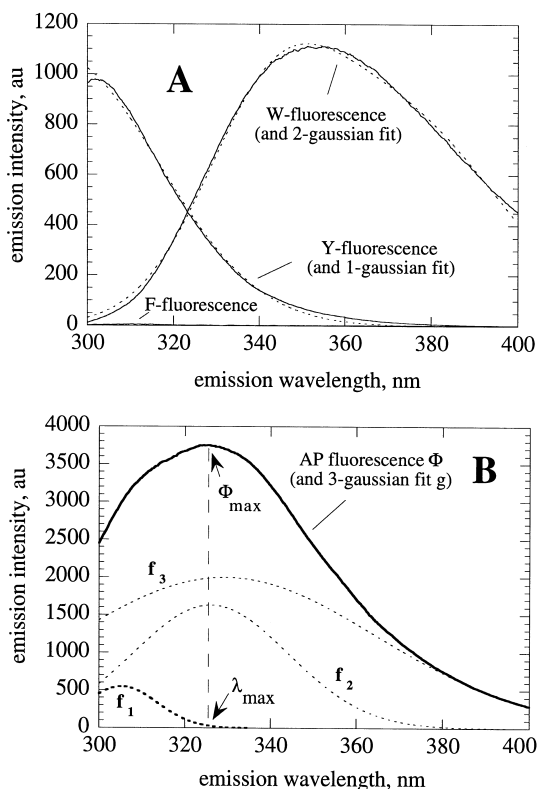


Fig. 5. (A) Emission spectra of tryptophan (W), tyrosine (Y) and phenylalanine (F) excited at  $\lambda_{\text{ex}} = 280$  nm, pH 7.5. Dashed lines show the curve fits of a single gaussian function ( $f_i$ , Eq. (5)) to the Y-fluorescence and a 2-gaussian function  $f_k + f_j$  to the W-fluorescence. (B) Average AP emission spectrum  $\Phi$  from 25 single scans and its decomposition into the three gaussian functions  $f_1, f_2, f_3$  (storage pH 7.5). Scan speed 1200 nm/min, at  $\lambda_{\text{ex}} = 280$  nm. Vertical dashed line indicates maximum emission  $\Phi_{\text{max}}$  at emission wavelength  $\lambda_{\text{max}}$ .

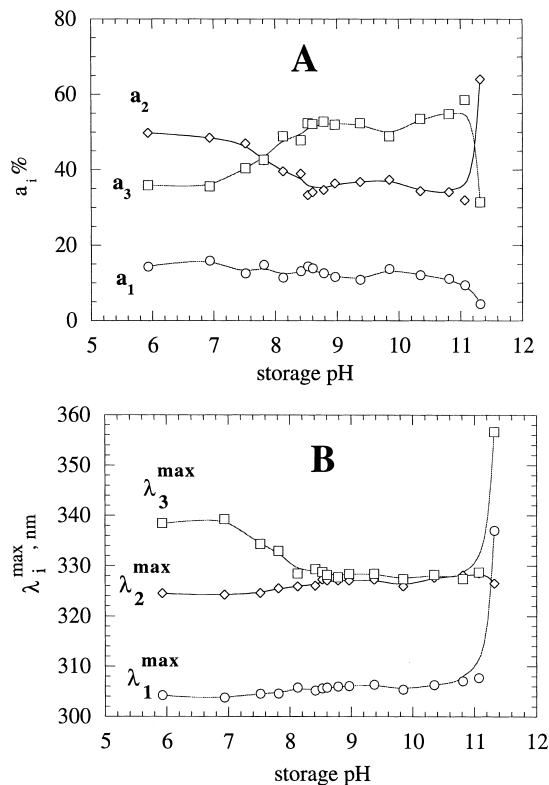
In the model's most simple form, reaction channels R1 and R3 are neglected ( $\alpha$  and  $\beta$  both zero) and the pH-optimum can be described as

$$\text{pH}_{\text{opt}} = \frac{1}{2}(pK_A^E + pK_A^{ES}) - \frac{1}{2} \log \left( \frac{K_M K_B^E + [S] K_B^{ES}}{K_M K_A^E + [S] K_A^{ES}} \right) \quad (7)$$

If  $K_A^{E(S)}$  and  $K_B^{E(S)}$  are of the same order of magnitude (or equal) the second term in Eq. (7) can be neglected. From this it can then easily be seen that an increase of the dissociation constants  $K_A^{E(S)}$ ,  $K_B^{E(S)}$  (a decrease in the corresponding

pK-values) will lead to a decrease in pH-optimum. For storage pH larger than 8.3 the  $pK_{A,B}^{E(S)}$  values decrease monotonically with increasing pH (with the exception of  $pK_A^E$ ) indicating an increase in these dissociation constants. An increase in storage pH is apparently one way to induce increased proton dissociation from the enzyme. The decrease of  $pK_{A,B}^{E(S)}$  is also accompanied by a decrease of  $\Phi_{\text{max}}$  (and an increase in  $\lambda_{\text{max}}$ ) as storage pH increases (Fig. 6D). However, we are presently not able to explain the somewhat more complicated behavior of  $pK_A^E$ .

The gradual increase of  $\lambda_{\text{max}}$  for increasing storage pH (Fig. 6D) is probably due to partial unfolding of the enzyme and, due to that, an increased interaction between solvent water and the fluorophore [20]. Due to the increased interaction between solvent and fluorophore, there is a corresponding general decrease in  $\Phi_{\text{max}}$ , probably due to quenching by dissolved oxygen. This possible quenching by dissolved  $O_2$  may be



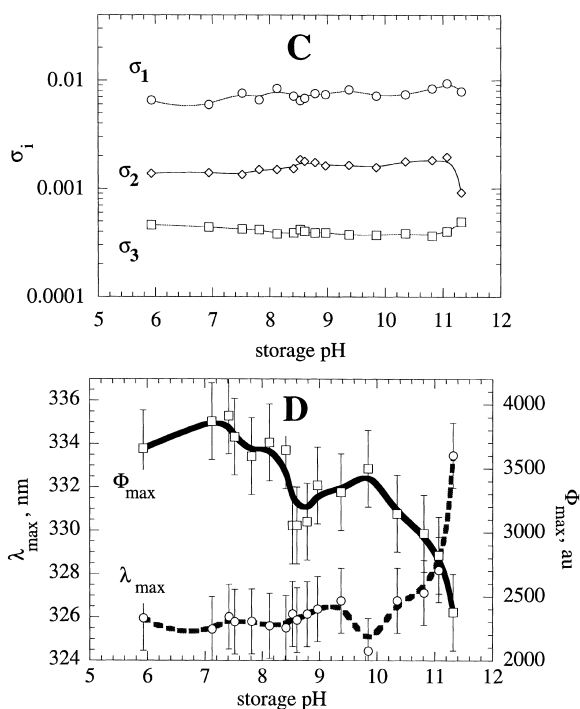


Fig. 6. (A)–(C) Variation of optimized  $a_i$ ,  $\lambda_i^{\max}$ , and  $\sigma_i$  values of  $g$  (Eq. (6)) as a function of storage pH. (D) Experimental  $\Phi_{\max}$  and  $\lambda_{\max}$  values as a function of storage pH. Average experimental uncertainties of  $\Phi_{\max}$  ( $\pm 350$  au) and  $\lambda_{\max}$  ( $\pm 1.5$  nm) are indicated.

one source of the rather large experimental variations observed for  $\Phi_{\max}$  (Fig. 6D). Another possibility to explain these large variations in  $\Phi_{\max}$  and  $\lambda_{\max}$  may be due to structural fluctuations of the enzyme [21].

Because AP works at the diffusion-controlled limit [10], we may assume that ionization reactions are fast. In the diprotic model this is reflected by the rapid equilibrium assumption of the protonization/de-protonization reactions. However, the dissociation constants will depend on the enzyme's conformation, which again will, among other parameters, be a function of environmental pH. The time scales of conformational changes or protein folding range from extremely fast elementary processes to exceedingly slow reactions [22]. However, in our case the time scale of conformational rearrangement, for example during an assay, must be slower than our assay time of 400 s.

Fig. 7 shows the time scale of the activity adaptation (hysteresis) when storage pH is changed from pH 10.0 to pH 7.3 (see Section 2.3 for experimental details). It was found that the adaptation can be described as a 1st-order process with a relaxation time of approximately 2 h. If the conformational rearrangement would be more rapid than the assay time, the pH-optimum would reflect the enzyme's conformation at assay pH and should therefore be independent of storage pH. Therefore in the AP and NR systems the pH-optimum reflects the enzyme's conformation in the storage buffer, which will change only slowly during the assay time. Due to this slow time response of the conformational rearrangement in the assay, AP and NR can be considered to have hysteretic properties [23,24]. Indeed, NR has been shown to be a hysteretic enzyme [25].

Ricard et al. [26,27] have proposed a theoretical model for pH-induced cooperative effects in hysteretic enzymes. Interestingly, this model predicts that the pK of an ionizable group is changed upon a conformational transition induced by pH!

Fowler and Walmsley [28] found during clinical quality control of commercial AP-sera that different sera showed quite substantial differences in pH-optimum, ranging from 9.75 up to 10.25.

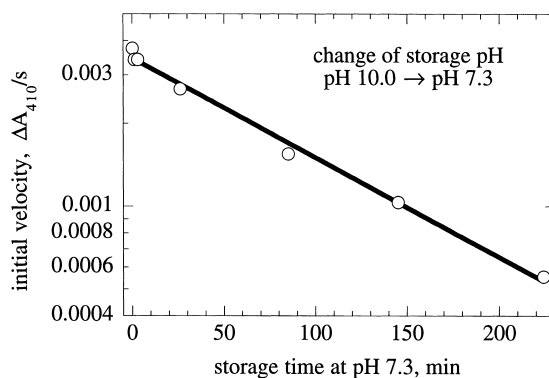


Fig. 7. Logarithm of initial velocities as a function of storage time when storage pH is changed from pH 10.0 to pH 7.3. Linearity of the plot suggests that the decrease in velocity is a 1st-order process with a relaxation time of approximately 2 h. The solid line represents the exponential fit  $y = 0.003453 \times \exp(-0.0083265 t)$  ( $R = 0.9945$ ) where  $y$  is initial velocity and  $t$  is storage time.

Although these sera came from different commercial suppliers and may, a priori, have different pH-optima, a possible reason of these differences may have been different storage buffers suggested by the manufacturers.

There is the question how general such an inverse relationship between pH-optimum and environmental pH actually is. It is apparently independent of the type of buffer used, as this inverse relationship is also observed in phosphate buffer [9]. Although we believe that other hysteretic enzymes may show an inverse relationship between pH-optimum and storage pH, there will also be systems with alternative types of responses. For example, preliminary results from wheat germ acid phosphatase (Sigma; using the same substrate as in this study) showed that an increase in storage pH does not alter the pH-optimum ( $\approx 7$ ) observed, but a new shoulder/peak at even more acid assay pH ( $\approx 4.5$ ) appeared. For high storage pH, the activity of the new shoulder became as large as the original pH-optimum. When the substrate has different ionic forms that may bind differently with the ionic forms of the enzyme, even more complicated response patterns may arise.

## 5. Conclusion

The pH-optimum of alkaline phosphatase changes reversibly in opposite direction to pH changes of storage buffer. With an increase of storage pH an increase of the proton dissociation constants in the diprotic model are observed. In addition,  $\lambda_{\max}$  and  $\Phi_{\max}$  increases and decreases, respectively. Both increase in dissociation constants and the change of  $\Phi_{\max}$  and  $\lambda_{\max}$  can be interpreted by a gradually more 'open' conformation of AP at storage conditions. This conformation adapts only slowly to the pH condition in the assay. The inverse relationship between pH-optimum and storage pH is expected to occur also for other enzymes whenever an increase in storage pH allows for a slow (hysteretic) conformational change that increases the dissociation of activity-related protons.

At  $\lambda_{\text{ex}} = 280$  nm the fluorescence of AP can be described with high precision as the sum of three

gaussian functions, one describing the putative tyrosine fluorescence, while the other two describe the tryptophan fluorescence.

## Acknowledgements

This work was supported by a grant from the Norwegian Academy of Sciences (Nansenfondet).

## References

- [1] L. Michaelis, H. Davidsohn, *Biochem. Z.* 35 (1911) 386.
- [2] S.G. Waley, *Biochim. Biophys. Acta* 10 (1953) 27.
- [3] R.A. Alberty, V. Massey, *Biochim. Biophys. Acta* 13 (1954) 347.
- [4] I.H. Segel, *Enzyme Kinetics, Behavior and Analysis of Rapid Equilibrium and Steady State Enzyme Systems*. Wiley, New York, 1975, p. 884.
- [5] K.F. Tipton, H.B.F. Dixon, Effects of pH on enzymes, in: D.L. Purich (Ed.), *Methods of Enzymology*, vol. 63A, Academic Press, New York, 1979, p. 183.
- [6] A. Cornish-Bowden, *Fundamentals of Enzyme Kinetics*, Portland Press, London, 1995, p. 187.
- [7] W.W. Cleland, Determining the chemical mechanisms of enzyme reactions by kinetic studies, in: A. Meister (Ed.), *Advances in Enzymology*, vol. 45, John Wiley, New York, 1977, p. 273.
- [8] A. Cornish-Bowden, *Principles of Enzyme Kinetics*, Butterworth, London, 1976, p. 108.
- [9] P. Ruoff, C. Lillo, *Biophys. Chem.* 67 (1997) 59.
- [10] T.T. Simopoulos, W.P. Jencks, *Biochemistry* 33 (1994) 10375.
- [11] R. Han, J.E. Coleman, *Biochemistry* 34 (1995) 4238.
- [12] E.E. Kim, H.W. Wyckoff, *Clin. Chim. Acta* 186 (1989) 175.
- [13] E.E. Kim, H.W. Wyckoff, *J. Mol. Biol.* 218 (1991) 449.
- [14] E. Moessner, M. Boll, H.E. Pfeleiderer, *Hoppe-Seyler's Z. Physiol. Chem.* 361 (1980) 543.
- [15] A. Cornish-Bowden, C.W. Wharton, *Enzyme Kinetics*, IRL Press, Oxford, 1988, p. 13.
- [16] W.H. Press, B.P. Flannery, S.A. Teukolsky, W.T. Vetterling, *Numerical Recipes (Fortran Version)*. Cambridge University Press, Cambridge, 1989, p. 302.
- [17] H. Weissig, A. Schildge, M.F. Hoylaerts, M. Iqbal, J.L. Millán, *Biochem. J.* 290 (1993) 503.
- [18] J.M. Beechem, L. Brand, *Annu. Rev. Biochem.* 54 (1985) 43.
- [19] T.C. Stadtman, Alkaline phosphatases, in: P.D. Boyer, H. Hardy, K. Myrbäck (Eds.), *The Enzymes*, vol. 5, Academic Press, New York, 1961, p. 55.
- [20] K.E. van Holde, W. Curtis Johnson, P. Shing Ho, *Physical Biochemistry*, Prentice Hall, Upper Saddle River, NJ, 1998, p. 461.
- [21] G.R. Welch, *The Fluctuating Enzyme*, Wiley, New York, 1986.

- [22] R. Rudolph, G. Böhm, H. Lilie, R. Jaenicke, Folding proteins, in: T.E. Creighton (Ed.), *Protein Function. A Practical Approach*, IRL Press, Oxford, 1997, p. 57.
- [23] C. Frieden, *Annu. Rev. Biochem.* 48 (1979) 471.
- [24] K.E. Neet, G.R. Ainslie Jr., Hysteretic enzymes, in: D.L. Purich (Ed.), *Methods of Enzymology*, vol. 64, Academic Press, New York, 1980, p. 192.
- [25] C. Lillo, P. Ruoff, *J. Biol. Chem.* 267 (1992) 13456.
- [26] J. Ricard, G. Noat, J. Nari, *Eur. J. Biochem.* 145 (1984) 311.
- [27] J. Nari, G. Noat, J. Ricard, *Eur. J. Biochem.* 145 (1984) 319.
- [28] R.T. Fowler, T.A. Walmsley, *Clin. Chim. Acta* 87 (1978) 159.